Queues and Artificial Potential Trenches for Multirobot Formations

Shuzhi Sam Ge, *Senior Member, IEEE,* and Cheng-Heng Fua, *Student Member, IEEE*

***Abstract*—In this paper, we present a novel approach for representing formation structures in terms of queues and formation vertices, rather than with nodes, as well as the introduction of the new concept of artificial potential trenches, for effectively controlling the formation of a group of robots. The scheme improves the scalability and flexibility of robot formations when the team size changes, and at the same time, allows formations to adapt to obstacles. Furthermore, for multirobot teams to operate successfully in real and unstructured environments, the instant goal method is used to effectively solve the local minima problem.**

***Index Terms*—Artificial potential trenches, coordination, formations, multirobots, queues.**

I. Introduction

In RECENT years, architectures such as ALLIANCE [1], MURDOCH [2], and BOAs [3], have been proposed for coordinating robots in unstructured environments. For robot formation maneuvers in highly unstructured environments (e.g., unmanned surveillance) where team size may change unexpectedly, it is important to consider formation scalability and flexibility. Social potentials [4], using a predetermined set of "attachment sites" around each robot, has been proposed to increase scalability. However, it offers no control over a formation's geometry, and formations, such as the wedge, cannot be achieved. A distributed approach, relying on communications, has been proposed to handle unexpected obstacles and to achieve coordinated motion in a linear pattern [5]. Social roles [6], assigned by a dynamically chosen leader, may also be used to cope with changes in the team. General methods for designing controllers have also been proposed for robots moving along a desired path and with fixed robot-to-formation-node assignments [7].

Although centralized control has been used successfully [8], by relying only on one computing and command center, centralized control is prone to failure especially in dynamic and uncertain environments. Thus, decentralized control has been a popular approach for several schemes. Virtual leaders [9] have been proposed for herding the robots into desired formations. Specific robot identifications (IDs) have been used in several schemes [10]–[12], where each robot is associated with, and required to track, a predefined position in the formation. In [13], a formation constrained function was used to determine the team formation that moves along a specified path. The virtual structure approach [14] has also been proposed for formation control. To improve coordination and individual fuel consumption

TABLE I
Nomenclature

$\mathbb{R}$	the field of real numbers;
$\mathbb{R}^{n\times m}$	the set of $n \times m$-dimensional real matrices;
$\mathbf{x}$	a vector expressed in the world coordinate frame;
$\hat{\mathbf{x}}$	the unit vector of a vector $\mathbf{x}$;
$\mathbf{x}_{(f)}$	a vector $\mathbf{x}$ expressed in the frame f. Taken to be in the world frame if unspecified;
$g_{(f)}(\cdot)$	a function $g(\cdot)$, expressed in the frame f;
$\|\mathbf{x}\|, x$	the Euclidean norm of a vector $\mathbf{x}$;
$\mathbf{T}_{(f_1)}^{(f_2)}$	the transformation matrix from frame f_1 to f_2;
R_{jk}	the jk-th element of a matrix $\mathbf{R}$;
$\otimes$	the vector product operator;
$\|\mathrm{X}\|$	the cardinality of a set X;
r_i	robot i;
$\mathcal{Q}$	the set of all the queues in a formation $\mathcal{F}$;
$\mathcal{G}$	the set of all the formation vertices;
$\mathcal{Q}_j$	the j-th queue in the set $\mathcal{Q}$;
$\mathcal{V}_j$	a list of (either one or two) formation vertices that influences $\mathcal{Q}_j$;
$\mathcal{S}_j$	the set of points describing the shape of $\mathcal{Q}_j$;
$\mathcal{C}_j$	the capacity $\in [0, 1]$ of $\mathcal{Q}_j$;
$\mathcal{E}_j$	the encapsulating region of $\mathcal{Q}_j$;
$\chi_i(t)$	is the queue status of r_i at t;
E_j	excess length (the number of excess robots in Q_j);
$\mathbf{q}_i, \mathbf{q}_t$	position of robot i and target respectively;
$\mathbf{v}_i, \mathbf{v}_t$	velocity of robot i and target respectively;
$\boldsymbol{\kappa}_i, \boldsymbol{\kappa}_t$	(topside-vector) vector normal to the plane of robot i and target respectively;
$\mathbf{q}_{(vj),i,nr}$	the vector from a robot r_i at $\mathbf{q}_{(vj),i}$ to the nearest point on its queue $\mathcal{Q}_j$ at $\mathbf{q}_{(vj),nr}$;
$\mathbf{x}_{(f),i,t}$	the relative position ($\mathbf{x} = \mathbf{q}$), velocity ($\mathbf{x} = \mathbf{v}$) or topside-vector ($\mathbf{x} = \boldsymbol{\kappa}$) of target w.r.t. r_i in frame f;
$\ell_{j,i,nr}$	the shortest distance between r_i and a queue $\mathcal{Q}_j$;
N_{tot}	the number of robots currently in the team;
N_v, N_q	the number of formation vertices and queues respectively;
ρ_{sf}	the safety distance between r_i and an obstacle;
ρ_{adp}	the distance a deformed queue is from an obstacle;
ρ_0	the influence range of an obstacle;
R_{max}	the maximum range of r_i's range sensor;
R_{act}	($\leq R_{max}$), the active range of the Instant Goal behavior;
$\mathbf{n}_{R,t}$	the unit vector of the ray from the range readings that is closest to $\hat{\mathbf{q}}_{(ri),i,t}$;
(ϕ, θ)	a pair representing the direction of an arbitrary point in the frame of r_i.
$U^b, \mathbf{F}^b$	the potential function and force derived for a behavior b;
F^b	the magnitude of the force $\mathbf{F}^b$;
a_b	the weighting parameter for a behavior b;
δ, δ_a	the average distance of robots from their queues and deformed queues (if applicable) respectively;
$c_{ig,on}$	ON(1)/OFF(0) status of Instant Goal Behavior;
v_{max}, ω_{max}	the maximum speed and turnrate of a robot respectively.

Manuscript received June 21, 2004; revised November 26, 2004. This paper was recommended for publication by Associate Editor L. Parker and Editor S. Hutchinson upon evaluation of the reviewers' comments. This paper was presented in part at the IEEE International Conference on Robotics and Automation, New Orleans, LA, April 2004.

S. S. Ge is with the Electrical and Computer Engineering Department, National University of Singapore, 117576 Singapore (e-mail: elegesz@nus.edu.sg).

C.-H. Fua is with the Graduate School for Integrative Sciences and Engineering, National University of Singapore, 117576 Singapore (e-mail: c.fua@nus.edu.sg).

Digital Object Identifier 10.1109/TRO.2005.847617

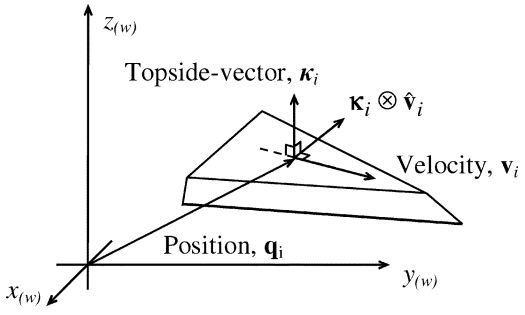

Fig. 1. Vectors $\mathbf{q}_i, \mathbf{v}_i$, and $\boldsymbol{\kappa}_i$ of r_i (or the target) in the world coordinate system.

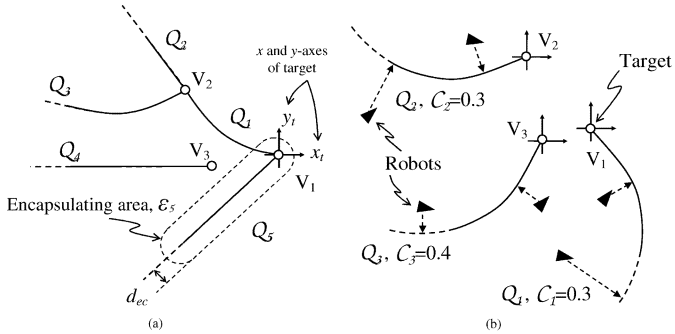

Fig. 2. Examples of queues, and formation vertices (circles), where x_t and y_t are the axes of the coordinate frame of the target centered at V_1. Open queues are drawn with solid (and dashed) lines, indicating that they extend indefinitely from the vertex. (a) Queues and vertices. (b) Robots (black triangles) entering their queues on a two-dimensional plane.

efficiency, the computation of the team's virtual center is proposed in [15]. For formations where strict rigidity is required, nodes/edges of graphs may be added and removed dynamically in response to the addition/removal of robots [16]. Formation stability is another important issue that has been investigated by several researchers [17]–[19].

The main contributions of this paper are as follows. First, the concept of queues, instead of nodes, is proposed as a novel and flexible methodology to define and support a large variety of formations. A decentralized redistribution algorithm is used for robots to redistribute themselves dynamically amongst queues, in response to changes in the formation or in the number of robots in the team. Furthermore, conventional methods using potential fields, which attract robots to predetermined points in order to form the desired pattern, limit the formation's scalability. We generalize this to a line using the artificial potential trench, each associated with a queue. Each robot will be attracted to, and will move along the bottom of the "valley" created by the potential trench, automatically distributing themselves along the trench. Preliminary results of this research was presented in [20].

II. Emergent and Self-Organizing Formations: Queues and Artificial Potential Trenches

Before proceeding further, the following assumptions are made in this paper.

Assumption 1: Each robot is able to broadcast information to others. The wireless communication has a limited range and is not assumed to be perfect, i.e., links may be broken.

Assumption 2: The team follows a target (either virtual or real), and the position $\mathbf{q}_t \in \mathbb{R}^3$, velocity $\mathbf{v}_t \in \mathbb{R}^3$, and topside orientation vector $\boldsymbol{\kappa}_t \in \mathbb{R}^3$ of the target are known, with $\|\mathbf{v}_t\| < v_{\max}$. The unit vector $\boldsymbol{\kappa}_t$ is normal to the top surface of the target, and together with $\mathbf{v}_t$ specifies the overall orientation of the target, as shown in Fig. 1.

Assumption 3: A robot r_i is able to estimate its position $\mathbf{q}_i, \mathbf{v}_i$, and $\boldsymbol{\kappa}_i$ (with the convention in Fig. 1) in the world coordinate system.

A. Formations and Queues

In practical applications, formations usually take the form of geometric shapes, which may be conveniently subdivided into a series of smooth line segments. Each of these line segments are referred to as *queues*. The proportion of all of the N_{tot} robots in the team to be allocated to each queue for each formation is specified by the user and may be changed during runtime when the need arises. This increases the flexibility of formations, which scales according to changes in N_{tot}, since proportions are used instead of exact numbers.

Definition 2.1 (Formations): A formation is denoted by $\mathcal{F} = (\mathcal{Q}, \mathcal{G}(N_{\text{tot}}))$, where $\mathcal{Q}$ is the set of all of the queues that make up the formation,[1] and $\mathcal{G}(N_{\text{tot}})$ represents the set of formation vertices, V_i $(i = 1, \ldots, N_v)$,[2] around the target.

The positions of the formation vertices may be specified such that they scale proportionally with N_{tot} and thereby avoid having an arbitrarily densely packed queue. For instance, assuming that $V_2 = (-4, 5)$ in Fig. 2(a) is specified for a team of $N_{\text{tot},0}$ robots, V_2 may be rewritten as $V_2 = (N_{\text{tot}})/(N_{\text{tot},0})(-4, 5)$. Formation vertices do not uniquely define the appearance of a formation. They merely represent a minimal number of pertinent locations in a formation and pure examination of the formation vertices do not yield complete information about what the formation looks like. As such, two different formations, such as the ones in Fig. 2, may have the same $\mathcal{G}(N_{\text{tot}})$. The actual appearance of the formation is mainly specified by the queues.

Definition 2.2 (Queues): A queue, $\mathcal{Q}_j \in \mathcal{Q}$, is denoted as $\mathcal{Q}_j = (\mathcal{V}_j, \mathcal{S}_j, \mathcal{C}_j, \mathcal{E}_j(N_{\text{tot}}))$. The four elements characterizing a queue are described as follows.

$\mathcal{V}_j \subseteq \mathcal{G}(N_{\text{tot}})$ (queue vertices): a list of (one or two) formation vertices through which $\mathcal{Q}_j$ passes.

$\mathcal{S}_j$ (shape): a set of points following an equation in $\mathbb{R}^3$ that describes the spatial appearance of $\mathcal{Q}_j$, and is specified in the coordinate frame of the first formation vertex in $\mathcal{V}_j$.

$\mathcal{C}_j$ (capacity): a fraction that refers to the proportion of all of the robots in the formation it can hold, i.e., $\sum_{j=1}^{N_q} \mathcal{C}_j = 1$, where N_q is the total number of queues in the formation.

$\mathcal{E}_j$ (encapsulating region): the set of points within a certain distance d_{ec} of the queue. The region is dependent on the

[1]Note that when the number of robots is too small (i.e., $\leq N_v$, the number of formation vertices), the robots will all be located at the vertices, and the scheme becomes highly similar to strategies using node-to-robot formation structures. However, in such a case, the robots are not able to reasonably form up into the desired formation no matter what scheme is used (e.g., two robots trying to form a wedge formation).

[2]Each formation vertex is represented by its position relative to the coordinate frame of the target.

number of robots that should reside on the queue and is hence related to N_{tot}.[3]

Queues may further be classified into *closed* and *open* queues. This characteristic influences the constraints on the shape of the queues.

Definition 2.3 (Closed Queues): Closed queues are those that have two formation vertices in $\mathcal{V}_j$. The curve describing $\mathcal{S}_j$ is constrained to pass through the second vertex in $\mathcal{V}_j$ [e.g., $\mathcal{Q}_1$ in Fig. 2(a)]. As the formation reaches steady state, all robots residing on a closed queue $\mathcal{Q}_j$ will be on the part of $\mathcal{Q}_j$ that are between the two vertices.

Definition 2.4 (Open Queues): Open queues are able to extend to infinity starting from the formation vertex in $\mathcal{V}_j$ that contains only one element.

Formations, such as the wedge and line formations, involve open queues, while some others, such as the diamond and circle, consist of closed queues. Fig. 2(a) shows an arbitrary formation that consists of five queues together with the corresponding queue capacities, in the coordinates of the target. The formation vertices (small circles, V_1, V_2, and V_3) are also reflected. In the figure, $\mathcal{Q}_2$ and $\mathcal{Q}_3$ share the same vertex. Queue 1 is a closed queue (with $\mathcal{V}_1 = \{V_1, V_2\}$), starting at V_1 and ending at V_2, while the rest are classified as open queues. Fig. 2(b) shows a formation with three queues and six robots (black triangles), each attracted to the nearest point in its respective queues.

Remark 2.1: For schemes based on nodes and edges, when formations are complex, it becomes difficult to track how the formation definition changes in response to the many different cases when team size changes, e.g., due to robot failures or additions. In the proposed scheme, the definition of a formation (usually specified by a higher level decision maker, possibly a human user) is independent of the reshuffling and adaptation of the formation, hence facilitating human–robot interactions. However, note that "node-to-robot" (NR) schemes have applications in areas which require strict adherence of each robot to specific points in the graph (e.g., grasping and transportation tasks by robotic fingers). On the other hand, there are also many applications (e.g., during pursuit, encirclement, and convoy movement) in which flexibility (and the formation's shape) is more important than rigidity, and for which the proposed scheme is highly suited.

B. Changing Queues

Given a formation, each robot has to dynamically decide the queue that it has to enter, in response to changing circumstances, e.g., when the total number of robots changes. Let $N_j = \text{Nearest Integer}(\mathcal{C}_j N_{\text{tot}})$ be the number of robots allowed in $\mathcal{Q}_j$, and $\chi_i(t)$ be the queue status[4] of r_i at time t. The robots are first randomly initialized such that they belong to one of the queues in the current formation. A robot i in queue j continually broadcasts its 1) distance (d_{ij}) from the first formation vertex in $\mathcal{V}_j$, and 2) queue status, to the other robots within the broadcast range. From the data broadcasted by the other robots, the following information may be derived by each robot.

1) The current number of robots in $\mathcal{Q}_j$, given by $N_{j,0}$, as well as N_{tot}.
2) The excess length of each queue in the formation, E_j. Excess length refers to the number of excess robots in the queue, e.g., in a queue with a capacity of 0.5, $E_j = N_{j,0} - 0.5N_{\text{tot}}$. Negative excess length means that the queue is not fully filled up.
3) The last member of each queue, defined by the robot in the queue that is the furthest from the corresponding queue vertex.

The queue evaluation process is decentralized and performed individually by each robot continuously over time. At every time step t, r_i currently in $\mathcal{Q}_j$ (i.e., $\chi_i(t) = j$) uses the following algorithm, and the most recent information it obtained from the broadcast channel (which may be subjected to network latencies) to arrive at a decision of its queue status for step $t+1$.

1: **for** $k = 1$ to N_q
2: Determine:

$$N_{k,0} = \sum_{h=1}^{N_{\text{tot}}} \begin{cases} 1, & \chi_h(t) = k \\ 0, & \text{otherwise.} \end{cases} \tag{1}$$

3: *// Any robot that lags too far behind the main team (due perhaps to equipment failure) will eventually move out of the team's broadcast range and be excluded.*
4: **if** $E_j \leq 0$ **then**
5: The current queue is either exactly full (and has no extra robots), or still has available space for more robots. No changes will be made to r_i's queue status.
6: **else**
7: **if** r_i is the last member of its queue **then**
8: The queue status will be modified as:

$$\chi_i(t+1) = \arg\min_{k \in \mathrm{E}^-} (\ell_{k,i,\text{nr}}) \tag{2}$$

where E^- is the set of all the queues with negative excess length, and $\ell_{k,i,\text{nr}}$ is the shortest distance between r_i and $\mathcal{Q}_k$. If more than one queue in E^- are equally near to r_i, one will be chosen at random.
9: **else**
10: r_i will retain its current queue status.

Robots in queues with (positive) excess lengths will move toward the nearest queue that has negative E. By allowing only the last robot in each overpopulated queue to change their queue status, the formation will not experience large reshuffling when many robots from an overpopulated queue rush to occupy the extra space in an underpopulated queue. Whenever queue switching occurs, at least one space in all of the underpopulated queues will be filled. When an underpopulated queue becomes overpopulated due to a high influx of robots from other queues, the algorithm ensures that only the extra robots (furthest from the queue vertex) switch queue. The number of robots which will potentially change queue will hence be less than that which had entered the queue. As such, the number of robots that are

[3]In a way, $\mathcal{E}_j$ provides a wrap around each queue, and, when the formation reaches its intended form, all robots should rightly be within the encapsulating region of their respective queues.

[4]It may also be the information (with time/communication lags) regarding the queue status of r_i that another robot r_{i*} has at time t.

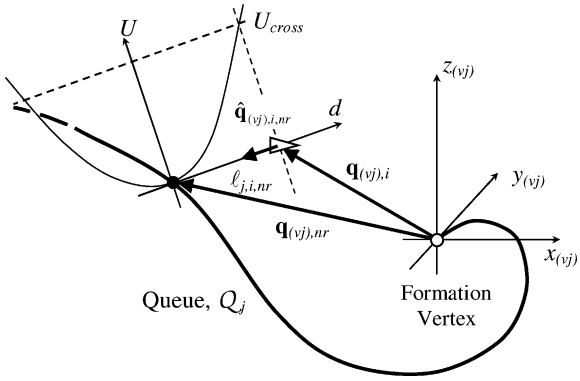

Fig. 3. Forces acting on a robot (r_i) when it enters a queue and the cross section of the potential trench. A robot is attracted to the point on $\mathcal{Q}_j$ (at $\mathbf{q}_{(vj),\mathrm{nr}}$) that is nearest to it.

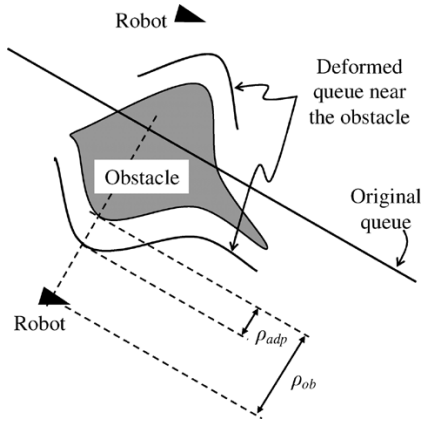

Fig. 4. Instead of the original queue (that passes through the obstacle), the presence of the obstacle causes the robots (triangles) to be attracted to the deformed queue that hugs the obstacle at a distance of ρ_{adp}.

eligible for changing queue will gradually decrease until all the queues reach full capacity.

Remark 2.2: In practical situations, certain robots may be disconnected from the team's communication network due to equipment malfunction or communication loss. New robots may also join the team. This causes the values of N_{tot} and E_j, that a robot computes, to change. The algorithm will dynamically redistribute the robots amongst the queues (based on $\mathcal{C}_j$ and computed values of N_{tot} and E_j), and scales the formation accordingly.

C. Potential Trench Functions

After a robot determines the queue to which it belongs, it will be attracted to the bottom of the artificial potential trench associated with that queue. The artificial potential trench for each queue may be synthesized with respect to the associated formation vertex such that it has the shape $(\mathcal{S}_j)$ of the queue. Robots in a potential trench will be attracted to the bottom of the trench.

Assuming that $\chi_i = j$, the following analysis is done in the coordinate system of the first formation vertex (at $\mathbf{q}_{vj}$ in the world frame) in the list $\mathcal{V}_j$. The x and z axes ($x_{(vj)}$ and $z_{(vj)}$) for this coordinate system are defined such that they coincide with the unit vectors of the velocity $(\hat{\mathbf{v}}_t)$ and topside orientation $(\boldsymbol{\kappa}_t)$ of the corresponding formation vertex, respectively. This can be seen more clearly from Figs. 1 and 2(b).

In general, let $g_{(vj)}$ be a function that defines the shape of $\mathcal{Q}_j$, which is continuously differentiable over the range in which the queue exists, and passes through all the formation vertices in the set $\mathcal{V}_{\mathcal{Q}}$. Furthermore, every point on the curve must be at a different distance from the origin. This ensures that for any point $\mathbf{q}_{(vj),i}$ in $\mathbb{R}^3$, there will be a point $\mathbf{q}_{(vj),\mathrm{nr}}$ on $g_{(vj)}$ that is nearest to $\mathbf{q}_{(vj),i}$. This is shown in Fig. 3. The point $\mathbf{q}_{(vj),\mathrm{nr}}$ can be obtained from

$$\mathbf{q}_{(vj),\mathrm{nr}} = \arg \min_{\mathbf{q}_{s1} \in Q_n} (\|\mathbf{q}_{s1}\|) \tag{3}$$

where Q_n is the set of points on the queue that satisfies $(\arg\min_{\mathbf{q}_s \in \mathcal{S}_j}(\ell_{Q_j}(\mathbf{q}_s)))$ with $\ell_{Q_j}(\mathbf{q}_s) = \|\mathbf{q}_s - \mathbf{q}_{(vj),i}\|$.

Let $U_{\mathrm{cross}}(d)$ describe the cross section of the potential trench, and let the shortest distance between the points $\mathbf{q}_{(vj),\mathrm{nr}}$ and $\mathbf{q}_{(vj),i}$ be given by $\ell_{j,i,\mathrm{nr}}$, as shown in Fig. 3. The cross section of the potential trench may be designed to take the form [21]

$$U_{\mathrm{cross}}(d) = a_{\mathrm{fm}} f(d) \tag{4}$$

where $f(d) = \sqrt{1+d^2} - 1$, d is the distance from the bottom of the trench, and the user defined parameter $a_{\mathrm{fm}} > 0$ determines the slope of the potential trench. Forces generated by such potentials have the advantage of being bounded and will not approach arbitrarily high values. Attractive potentials in the rest of this paper will adopt forms similar to $f(d)$. The differential of $f(d)$ with respect to scalar d is given by

$$f'(d) = \frac{d}{\sqrt{1+d^2}} = \frac{d}{f(d)+1}. \tag{5}$$

A robot at $q_{(vj),i}$ would be attracted to the nearest point $q_{(vj),\mathrm{nr}}$ on the queue, and the attractive force it experiences may be calculated as

$$\mathbf{F}^{\mathrm{fm}}_{(vj),i} = (\nabla_d U_{\mathrm{cross}}(d)|_{\ell_{j,i,\mathrm{nr}}})\hat{\mathbf{q}}_{(vj),i,\mathrm{nr}} \tag{6}$$

$$= f'(\ell_{j,i,\mathrm{nr}})\hat{\mathbf{q}}_{(vj),i,\mathrm{nr}} \tag{7}$$

derived in a similar manner as when conventional potential fields are used [22]. Note that the force is represented in the coordinate frame of the first vertex in $\mathcal{V}_j$.

1) Formation Adaptation and Deformation: When an obstacle is detected to be in the direction of $\hat{\mathbf{q}}_{(vj),i,\mathrm{nr}}$, r_i is attracted to the point that is before the obstacle, but still along the vector $\hat{\mathbf{q}}_{(vj),i,\mathrm{nr}}$. This can be seen more clearly in Fig. 4. In this case, the attractive force is modified to become

$$\mathbf{F}^{\mathrm{fm}}_{(vj),i} = (\nabla_d U_{\mathrm{cross}}(d)|_{\ell_{j,i,\mathrm{adp}}})\hat{\mathbf{q}}_{(vj),i,\mathrm{nr}} \tag{8}$$

where $\ell_{j,i,\mathrm{adp}}$ is given by

$$\ell_{j,i,\mathrm{adp}} = \begin{cases} \ell_{j,i,\mathrm{nr}}, & \text{no obstacles in the direction } \hat{\mathbf{q}}_{(vj),i,\mathrm{nr}} \\ \rho_{\mathrm{ob}} - \rho_{\mathrm{adp}}, & \text{otherwise} \end{cases} \tag{9}$$

and $\rho_{\mathrm{ob}} > 0$ is the distance along $\hat{\mathbf{q}}_{(vj),i,\mathrm{nr}}$ between r_i and the obstacle, and $\rho_{\mathrm{adp}} > \rho_{\mathrm{sf}}$ is the distance the deformed formation is to be from the obstacle, where ρ_{sf} is a safety distance between a robot and an obstacle.

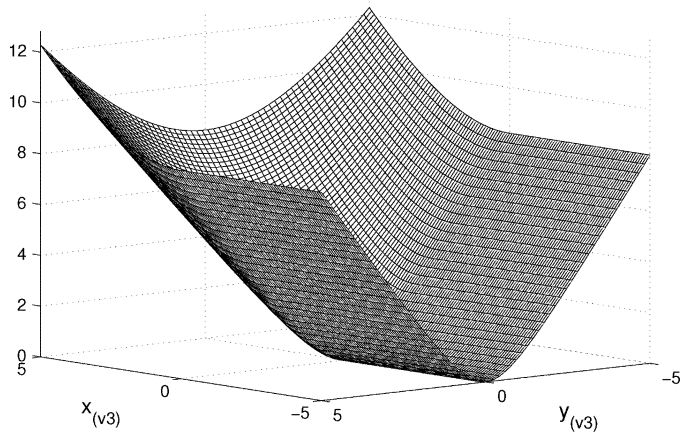

Fig. 5. Three-dimensional view of the potential trench function of Q_4 in the (x, y) coordinate space of the vertex, V_3.

For illustration, consider $\mathcal{Q}_4$ in Fig. 2(a), with the robots moving in $\mathbb{R}^2$. The potential trench experienced by a robot in $\mathcal{Q}_4$, at (x, y) in the frame of V_3, is given by

$$U^{\rm fm}_{(v3),i}(x,y) = \begin{cases} a_{\rm fm}(\sqrt{x^2+y^2+1}-1), & \text{for } x \geq 0 \\ a_{\rm fm}(\sqrt{y^2+1}-1), & \text{otherwise} \end{cases} \tag{10}$$

and is shown in Fig. 5 for $a_{\rm fm} = 2$.

Robots are affected only by the potential trenches associated to their own queues. The repulsive forces (described in Section III) between robots will ensure that the robots maintain a desired distance between each other in the potential trench. The forces in the frame of the vertex may then be converted into the world coordinate frame, in which all of the forces acting on r_i are calculated, as follows:

$$\mathbf{F}^{\rm fm}_i = \mathbf{T}^{(w)}_{(vj)} \mathbf{F}^{\rm fm}_{(vj),i} \tag{11}$$

where

$$\mathbf{T}^{(w)}_{(vj)} = (\hat{\mathbf{v}}_t \quad \boldsymbol{\kappa}_t \otimes \hat{\mathbf{v}}_t \quad \boldsymbol{\kappa}_t). \tag{12}$$

III. Robot Behaviors

A. Target Tracking

Each robot sets its target to be the first formation vertex in $\mathcal{V}$ of its queue. The target tracking potential function for r_i, based on the work in [23] that takes into account the position and velocity of the target, is specified as

$$U^{\rm tg}_i(\mathbf{q}_i, \mathbf{v}_i, \boldsymbol{\kappa}_i) = a_{\rm tg}(a_{\rm tg1} f(q_{i,t}) + a_{\rm tg2} f(v_{i,t}) + a_{\rm tg3} f(\kappa_{i,t})) \tag{13}$$

where the parameters $a_{\rm tg}, a_{\rm tg1}, a_{\rm tg2}, a_{\rm tg3} > 0$. The corresponding attractive force is

$$\begin{aligned} \mathbf{F}^{\rm tg}_i &= \nabla_{\mathbf{q}_i} U^{\rm tg}_i \hat{\mathbf{q}}_{i,t} + \nabla_{\mathbf{v}_i} U^{\rm tg}_i \hat{\mathbf{v}}_{i,t} + \nabla_{\boldsymbol{\kappa}_i} U^{\rm tg}_i \hat{\boldsymbol{\kappa}}_{i,t} \\ &= a_{\rm tg}(a_{\rm tg1} f'(q_{i,t}) \hat{\mathbf{q}}_{i,t} + a_{\rm tg2} f'(v_{i,t}) \hat{\mathbf{v}}_{i,t} \\ &\quad + a_{\rm tg3} f'(\kappa_{i,t}) \hat{\boldsymbol{\kappa}}_{i,t}). \end{aligned} \tag{14}$$

The parameters weight the relative importance between tracking the target's position, velocity, and orientation. For this paper, the values of $a_{\rm tg1}, a_{\rm tg2}, a_{\rm tg3}$ are chosen to be 1, 0.5, and 0.5, respectively. A detailed discussion of the effect the parameters have on robot behaviors may be found in [23].

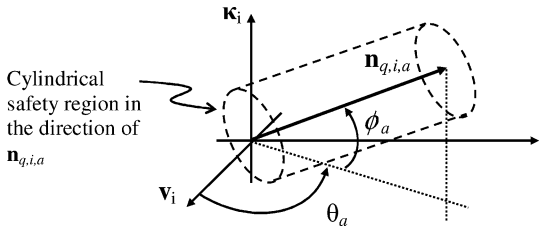

Fig. 6. Representation of the direction $(\mathbf{n}_{q,i,a})$ of a point in the coordinate frame of r_i by the pair (ϕ_a, θ_a).

B. Instant Goal (IG) Behavior

The IG method was first proposed in [24] to solve the local minima problem in robot path planning, through the use of dynamically created IGs. For completeness, the IG method, generalized for three-dimensional (3-D) spaces, is briefly described in this section.

It is assumed that r_i is equipped with range sensing equipment that is capable of producing a 3-D spherical scan. The direction of each reading (in the coordinate frame of r_i) is characterized by two angles $\phi \in [-90^\circ, 90^\circ], \theta \in (-180^\circ, 180^\circ]$ as shown in Fig. 6. In general, the direction of an arbitrary point in the frame of r_i may be represented by a pair (ϕ, θ). A matrix representation, $\mathbf{R} \in \mathbb{R}^{N_\phi \times N_\theta}$, of the range readings of r_i can then be obtained, where R_{jk} is the range return in the direction $(\phi(j), \theta(k))$ with $j = 1, 2, \ldots, N_\phi$ and $k = 1, 2, \ldots, N_\theta$ for

$$\begin{aligned} &\phi(j) = 90^\circ + (1-j)\phi_s, \quad \theta(k) = 180^\circ - (k-1)\theta_s \\ &N_\phi = \frac{180^\circ}{\phi_s} + 1, \quad N_\theta = \frac{360^\circ}{\theta_s} \end{aligned} \tag{15}$$

where ϕ_s and θ_s are the angular spacings between each reading. The pair (j, k) may also be seen as the representation of the direction of each range reading in $\mathbf{R}$. The unit vector (in r_i's coordinate frame) in the direction (j, k) is given by

$$\mathbf{n}_{(ri),(j,k)} = \begin{bmatrix} \cos\phi(j)\cos\theta(k) \\ \cos\phi(j)\sin\theta(k) \\ \sin\phi(j) \end{bmatrix}. \tag{16}$$

The angle between two pairs (j_1, k_1) and (j_2, k_2) is given by

$$\vartheta((j_1,k_1),(j_2,k_2)) = \cos^{-1}\left(\mathbf{n}^T_{(ri),(j_1,k_1)} \mathbf{n}_{(ri),(j_2,k_2)}\right). \tag{17}$$

Let (j_{ign}, k_{ign}) represent the direction of the IG that r_i chooses. In addition, let the directions of $\hat{\mathbf{q}}_{(ri),i,t}$ and $\mathbf{n}_{R,t}$ be given by (ϕ_t, θ_t) and $(\phi(j_R), \theta(k_R))$, respectively. The IG for r_i is determined as follows.

1: Find $(\phi(j_R), \theta(k_R))$, the ray closest to the target.
2: **if** $(R_{j_R k_R} \geq R_{\rm act}$ **and** $(-90^\circ \leq \theta_t \leq +90^\circ))$ **then**
3: *// r_i's target will be in its front hemisphere, i.e., the robot is deemed to be moving toward the target, and the path is possibly unobstructed. Turn off IG-behavior and check if a safe path exists.*

4: Set $c_{ig,on} = 0, F_i^{ig} = 0, (j_{ign}, k_{ign}) = (j_R, k_R)$.
5: **else**
6: **if** $c_{ig,on} = 0$ **then**
7: Set $(j', k') = (j_R, k_R)$.
8: **else**
9: Set the pair (j', k') to be the scanner ray that is closest to the previous IG.
10: Let (j_{ign}, k_{ign}) be the ray that is closest to (j', k'), and such that $R_{j_{ign}k_{ign}} \geq R_{\rm act}$ *and* at least one ray in its neighborhood has a range $< R_{\rm act}$.
11: Set $c_{ig,on} = 1$.
12: **if** (there is a cylindrical space in the direction (j_{ign}, k_{ign}) that is large enough for r_i to safely pass through) **then**
13: The position of the new IG in the coordinate frame of r_i is $\mathbf{q}_{(ri),i,ig} = R_{\max}\mathbf{n}_{(ri),(j_{ign},k_{ign})}$ with zero velocity, with topside-orientation $\boldsymbol{\kappa}_{i,\tau_i}$.
14: **if** r_i is in $\mathcal{E}_{\chi_i}$ **then**
15: Set $c_{ig,on} = 0$ to minimize disruption to formation.
16: EXIT
17: **else**
18: Set $R_{j_{ign},k_{ign}} = R_{\rm blk}$, where $0 < R_{\rm blk} \ll R_{\max}$ is a user defined constant.
19: GOTO Step 5.

In the world coordinate frame, the direction of the IG from r_i may be written as

$$\mathbf{n}_{i,ig} = \mathbf{T}_{(ri)}^{(w)}\mathbf{n}_{(ri),(j_{ign},k_{ign})} \tag{18}$$

where the transformation matrix is given by

$$\mathbf{T}_{(ri)}^{(w)} = (\hat{\mathbf{v}}_i \quad \boldsymbol{\kappa}_i \otimes \hat{\mathbf{v}}_i \quad \boldsymbol{\kappa}_i).$$

The force derived from the IG behavior F_i^{ig} is then obtained (similar to Section III-A) as follows, with $a_{ig} > 0$:

$$\mathbf{F}_i^{ig} = a_{ig}c_{ig,on}f'(R_{\max})\mathbf{n}_{i,ig}. \tag{19}$$

C. Obstacle Avoidance

Various obstacle avoidance techniques [10], [21] assume that the centers of the obstacles are known. However, in unstructured environments, such information may not be readily available. Sensor-based obstacle avoidance that takes velocity into account has been proposed [23]. Simple obstacle avoidance is implemented in this paper based on the range sensor returns. Let the repulsive potential in the direction represented by the pair (j, k) take the form of

$$U_{i,(j,k)}^{\rm ob}(R_{jk}) = \begin{cases} \frac{a_{\rm ob}}{R_{jk}}, & \text{for } 0 < R_{jk} < \rho_0 \\ 0, & \text{otherwise} \end{cases} \tag{20}$$

which yields the following repulsive force:

$$\mathbf{F}_{i,(j,k)}^{\rm ob}(R_{jk}) = -\frac{a_{\rm ob}}{R_{jk}^2}\mathbf{T}_{(ri)}^{(w)}\mathbf{n}_{(ri),(j,k)} \tag{21}$$

where ρ_0 is a positive constant, and $a_{\rm ob} > 0$ is a constant.

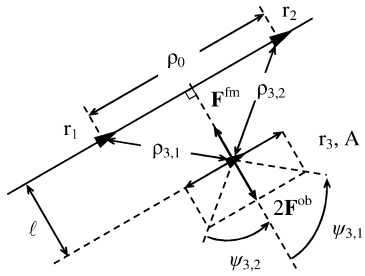

Fig. 7. Attractive and repulsive forces on a robot joining an established queue.

D. Overall Robot Behavior

The behavior of r_i may then be determined by the vector summation of all the individual forces derived in the earlier sections. This may be written as

$$\mathbf{F}_i^{\rm all} = \mathbf{F}_i^{\rm fm} + \sum_{j=1}^{N_\phi}\sum_{k=1}^{N_\theta}\mathbf{F}_{i,(j,k)}^{\rm ob} + \mathbf{F}_i^{\rm tg} + \mathbf{F}_i^{ig} \tag{22}$$

with user-defined parameters $a_{\rm fm}, a_{\rm ob}, a_{\rm tg}, a_{ig} > 0$.

IV. Analysis of Parameter Values

In this section, we discuss how the parameter $a_{\rm ob}$ in (21) should be chosen in relation to $a_{\rm fm}$ in (4) in order to avoid certain local minima conditions when robots attempt to join a queue. Consider the scenario in Fig. 7, in which r_3 tries to enter the queue in between r_1 and r_2. In this case, r_1 and r_2 are spread with a distance of ρ_0 due to the repulsive force between them. If the attractive force to the queue that r_3 experiences is not large enough to overcome the repulsive forces due to r_1 and r_2, a local minima will exist at point A. Robot r_3 will then be unable to join the queue, and subsequently move along the queue with the same velocity as the other robots residing on the queue.

Although obstacles temporarily disrupt the robots in the queue, when the team leaves the area around the obstacle, they will again be required to settle back into queue and the same local minima problem will still exist. Target tracking and IG behaviors are set to be relatively smaller than the formation and obstacle avoidance behaviors. Hence, for clarity, these behaviors will not be included in the following analysis. For $\rho_{3,1}, \rho_{3,2} > \rho_0, r_3$ will experience only attractive forces from the queue and will therefore move toward the queue. A problem only arises for $0.5\rho_0 \leq \rho_{3,1}, \rho_{3,2} \leq \rho_0$, and the attractive force from the queue balances the repulsive forces from the two neighboring robots. For notational simplicity, let $\rho = \rho_{3,1} = \rho_{3,2}$ and $\ell = \ell_{\chi_3,3,\rm nr}$. Accordingly, we have

$$0.5\rho_0 \leq \rho \leq \rho_0. \tag{23}$$

From geometry, we know that

$$\begin{aligned} \ell &= \rho\cos\psi \\ \frac{\pi}{6} &\leq \psi \leq \frac{\pi}{2}. \end{aligned} \tag{24}$$

Combining with the bounds on ρ, we obtain

$$0 \leq \ell \leq \frac{\sqrt{3}}{2}\rho_0. \tag{25}$$

Consider the magnitude of the forces along the straight line through point A perpendicular to the queue. The following analysis is carried out for a robot attempting to join the queue from one direction. Due to the symmetry of the potentials with respect to the queue, the same analysis applies if the robot is attempting to join the queue from other directions. From (5), (6), and (21), the magnitude of the obstacle repulsive and formation attractive forces may be written as

$$F_3^{\rm ob} = F_{3,1}^{\rm ob}(\rho) = F_{3,2}^{\rm ob}(\rho) = \frac{a_{\rm ob}\cos\psi}{\rho^2} \tag{26}$$

$$F_3^{\rm Fm} = \frac{a_{\rm fm}\ell}{\sqrt{1+\ell^2}}. \tag{27}$$

In order to allow r_3 to squeeze into the queue between r_1 and r_2, the formation force must be larger than the repulsive forces from r_1 and r_2, i.e.,

$$2F_3^{\rm ob} < F_3^{\rm Fm}. \tag{28}$$

This gives

$$\frac{a_{\rm ob}\cos\psi}{\rho^2} < \frac{a_{\rm fm}\ell}{2\sqrt{1+\ell^2}} \Rightarrow a_{\rm ob} < \frac{a_{\rm fm}\rho^3}{2\sqrt{1+\ell^2}}. \tag{29}$$

From the inequality in (25), we have

$$\frac{1}{\sqrt{1+0.75\rho_0^2}} \le \frac{1}{\sqrt{1+\ell^2}} \le 1. \tag{30}$$

Combining (23), (29), and (30), we obtain

$$a_{\rm ob} < \frac{0.125\rho_0^3\, a_{\rm fm}}{2\sqrt{1+0.75\rho_0^2}}. \tag{31}$$

In addition, $a_{\rm ob}$ should be lower bounded, so that the formation attractive force does not overwhelm the repulsive forces and cause collisions. Suppose that $a_{\rm ob} = \alpha a_{\rm fm}$ and satisfies (31). To prevent collisions, we let the repulsive force generated by an obstacle be equal to the maximum formation attractive force [which is a factor of $a_{\rm fm}$ due to the structure of the potential function in (4)] when the distance between the robot and the obstacle is $\rho_{\rm sf}$. This gives

$$\frac{\alpha a_{\rm fm}}{\rho_{\rm sf}^2} = \beta a_{\rm fm} \Rightarrow \alpha = \beta\rho_{\rm sf}^2 \tag{32}$$

where $\beta \ge 1$ is a user-defined constant. Therefore, by specifying $\rho_{\rm sf}, \alpha$ may be determined, and ρ_0 may be chosen in a way such that (31) is satisfied. In this way, for distances smaller than $\rho_{\rm sf}$, the repulsive force will be greater than the formation attractive force. This allows robots trying to join an already established queue to safely squeeze into a convenient point along the queue, and at the same time preventing robots from getting too close to each other.

V. Simulation Experiments

Realistic simulations are performed using the Player/Stage platform [25]. Let θ_f and θ_i (in degrees) be the angle of $\mathbf{F}_i^{\rm all}$ and r_i in the world coordinate system, respectively. The speed and turning rate of each differential drive robot is determined as follows [23]:

$$v_i = \min\left(K_s F_i^{\rm all}\cos(0.5(\theta_f-\theta_i)), v_{\max}\right) \tag{33}$$

$$\omega = \omega_{\max}(\theta_f-\theta_i)/180^\circ \tag{34}$$

where K_s is a positive constant. For the simulations $K_s = 0.1, v_{\max} = 100$ mm/s, and $\omega_{\max} = 30^\circ$/s. Range sensing is obtained from 32 sonar beams, equally spaced over 360°. The parameters used are given in Table II.

TABLE II
Parameter Values for Simulations

Parameters	a_{fm}	a_{ob}	a_{tg}	a_{ig}	ρ_0	ρ_{sf}
Value	10	2.5	1.5	2	2.15m	0.5m

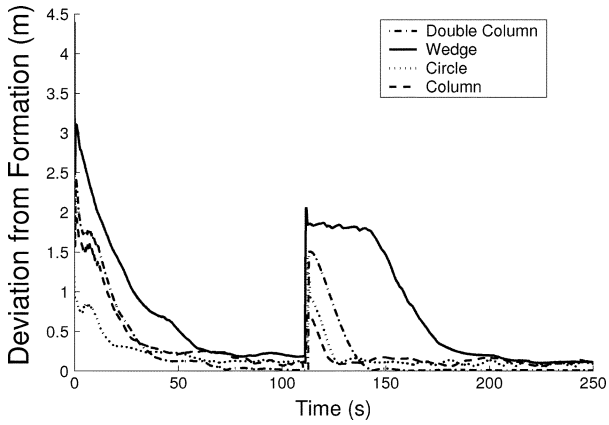

Fig. 8. Scaling of formations. Solid: wedge; dashed: column; dash–dot: double column; dotted: circle.

Four representative formations are used: 1) wedge (one vertex, two open queues); 2) column (one vertex, one open queue); 3) double column (two vertices, two open queues); and 4) circle (one vertex, two closed queues). To determine the closeness of a team of robots to a desired formation, the distance measure δ is used as follows:

$$\delta = \frac{1}{N_{\rm tot}}\sum_{r=1}^{N_{\rm tot}}(\ell_{\chi_i,i,{\rm nr}} + \ell_{\chi_i,i,E}) \tag{35}$$

where $\ell_{\chi_i,i,E}$ is the distance of the robot from the nearest point of the encapsulating area of the queue ($\mathcal{Q}_{\chi_i}$) to which it belongs. The distance δ may also be viewed as a form of error measure. Note that the distance of robots from their queues is, by itself, unable to provide a good measure of how closely the team has formed up into the desired formation, and must be used together with $\ell_{\chi_i,i,{\rm nr}}$. This is because robots may have already moved into the potential trench (resulting in very small $\ell_{\chi_i,i,{\rm nr}}$) before reaching the vicinity of the formation vertex.

Remark 5.1: Although regular formations are used, the concept may also be easily generalized for irregular formations. The difference is only in how the queues (or positions of nodes for NR-approaches) are specified for the two classes of formations. The main advantage of the proposed approach lies in its concise and flexible representation of formations that is independent of team size. This may be clearly brought out with commonly used formations (e.g., wedge). Consider the case when a team, in a double column formation, increases from 10 to

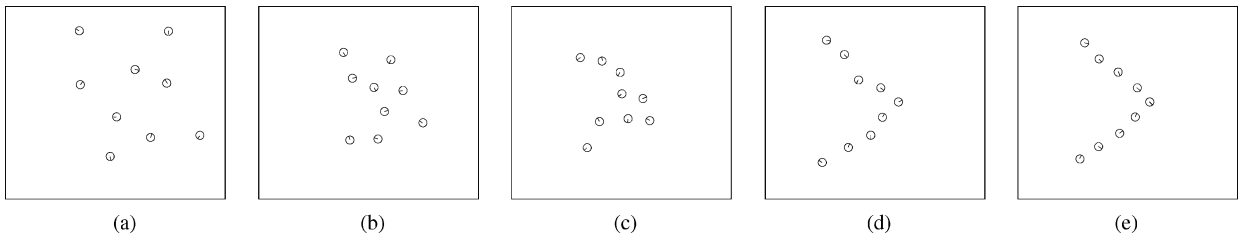

Fig. 9. Snapshots of the team of nine robots forming the wedge formation. (a) $t = 0$ s. (b) $t = 25$ s. (c) $t = 50$ s. (d) $t = 75$ s. (e) $t = 150$ s.

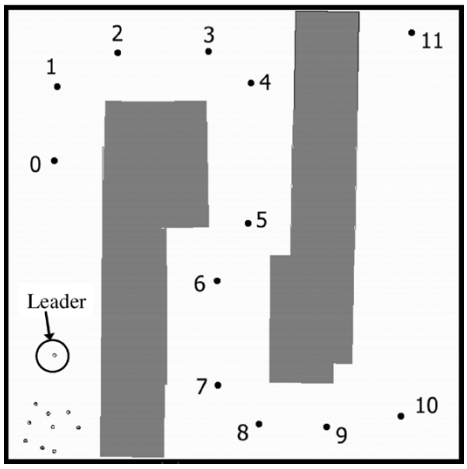

Fig. 10. Snapshot of corridor and waypoints.

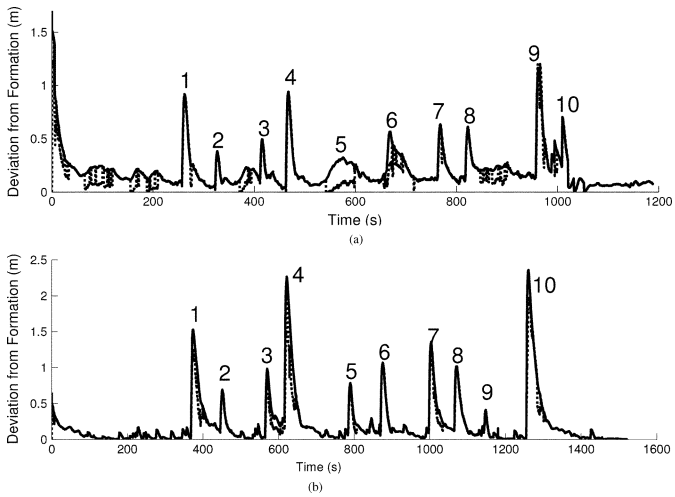

Fig. 11. Team maneuver through a confined corridor Solid: δ; dashed: δ_a. (a) Wedge formation movement. (b) Column formation movement.

30 robots. The proposed representation will always consist of two vertices and two open queues (regardless of team size), while NR-approaches require 20 nodes to be dynamically added and assigned. This observation is independent of whether the columns are straight or irregular lines.

A. Convergence to Formations and Scaling

The robots are initialized to random positions around a stationary target, and the value of δ against time is shown in Fig. 8. It is observed that δ decays to almost zero at $t \approx 100$ s. The graphs also show the effect a sudden reduction of robots (by half at $t \approx 110$ s). The robots are eventually able to scale the formation accordingly. Snapshots of the robots entering a wedge formation are shown in Fig. 9. Due to uncertainties, imperfection of the position data, and finite robot reaction times, δ never decays to exactly 0. The resulting average error is approximately 0.1–0.15 m. This is relatively small and does not greatly affect the team's overall formation.

B. Maneuvers in Confined Spaces

The team is required to follow a moving target (traveling at a speed of 0.6 ms^{-1} via a series of waypoints) through a winding corridor shown in Fig. 10. The graphs of δ against time for the column and wedge formations are shown in Fig. 11. To observe the effect of having adaptive queues, another distance measure

$$\delta_a = \frac{1}{N_{\text{tot}}} \sum_{r=1}^{N_{\text{tot}}} \left(\ell_{\chi_i, i, \text{adp}} + \ell_{\chi_i, i, E} \right) \tag{36}$$

is also used and is plotted as dashed lines in the graphs of Fig. 11. This measure is essentially the same as δ, except that it is dependent on the distance of the robot from the deformed queue and indicates how close the robots are to a deformed formation. By comparing the solid and dashed lines, the instances the formations adapt to nearby obstacles may be observed. Spikes in the graphs occur when the target (formation vertex) turns around the corners of the corridor. The turns and the corresponding spikes are numbered in Figs. 10 and 11. Milder turns resulted in lower spikes in the error graphs, and the wedge formation suffers larger deformations since it is laterally more spread out.

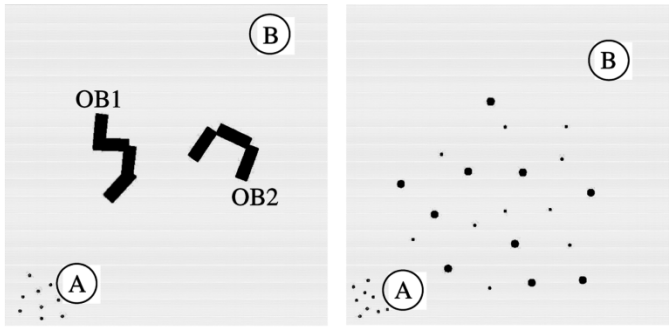

Fig. 12. Snapshot of environment with Type-I and -II obstacles. (a) Type-I obstacle field. (b) Type-II obstacle field.

C. Reaction of Formations to Obstacles

The robots are initialized to random positions near Point A and follows a virtual target, in a wedge formation, through an obstacle field to Point B, as shown in Fig. 12. Two types of obstacle fields are used: 1) Type I: large (more than ten times

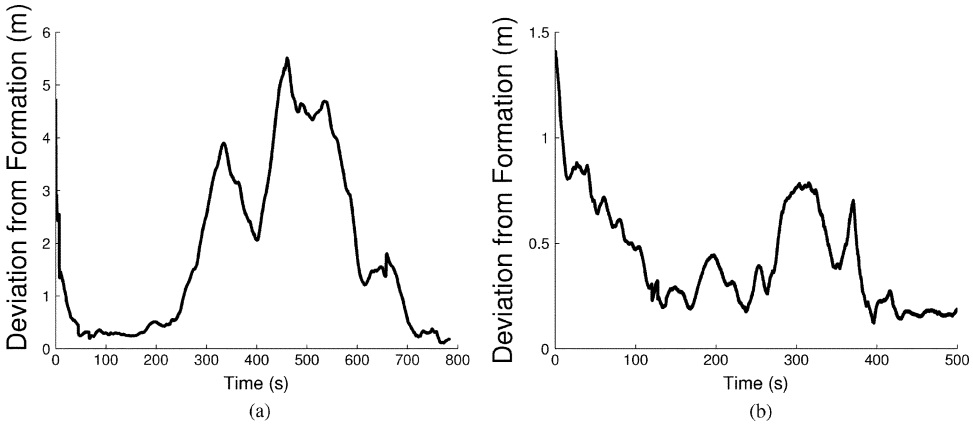

Fig. 13. Plot of δ versus time for team traversal through obstacle fields. (a) Type-I obstacles. (b) Type-II obstacles.

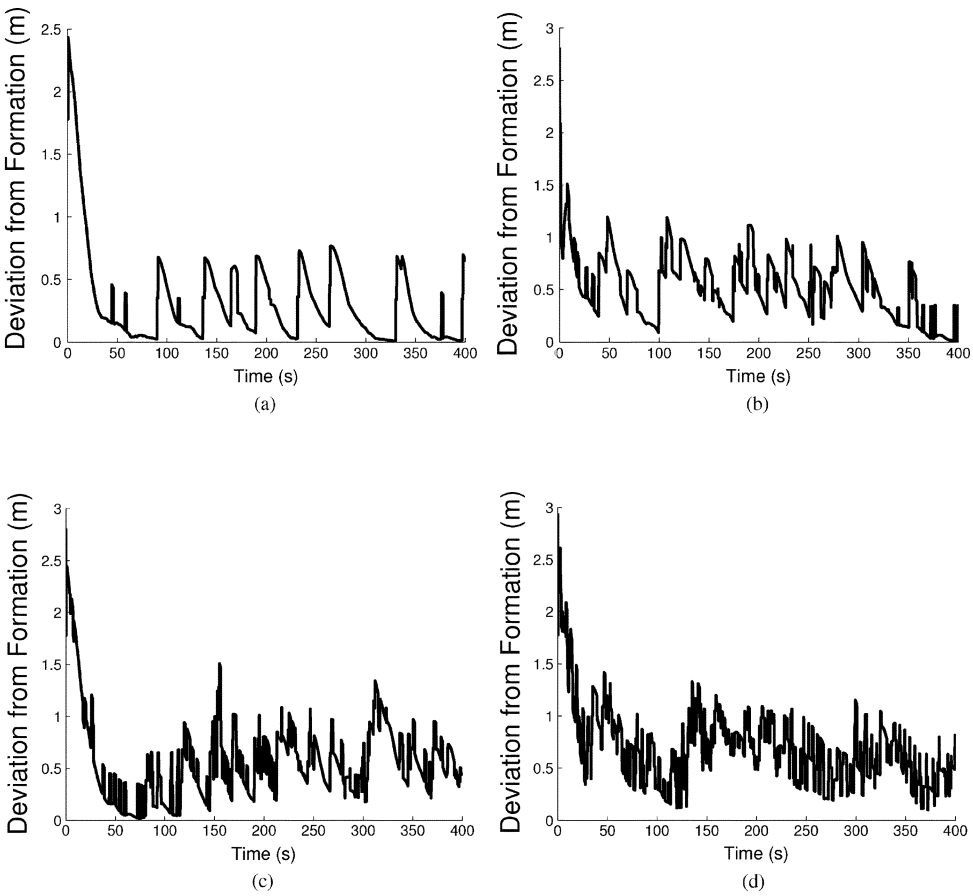

Fig. 14. Plot of δ versus time for disruption to a maximum of half the communications links. (a) $P_{\text{txloss}} = 0.05$. (b) $P_{\text{txloss}} = 0.25$. (c) $P_{\text{txloss}} = 0.50$. (d) $P_{\text{txloss}} = 1.0$.

the radius of each robot) and concave and 2) Type II: small (less than three times of each robot's radius) and convex. The effect Type-I and Type-II obstacles have on the team formation are shown in Fig. 13. The size and shape of the obstacles account for the error and amount of time required by the robots to maneuver around them. For both instances, the robots are able to return to their formation once they clear the obstacles.

D. Disruption of Wireless Communications

The formation errors (δ) when communication links between robots are disrupted with probability (P_{txloss}) of 5%, 25%, 50%, and 100%, are examined in this section. When this occurs, varying amounts of information (I_{loss}) is lost. In this section, the robot may lose up to a maximum of: 1) all $(I_{\text{loss}} = 1.00)$; 2) half $(I_{\text{loss}} = 0.50)$; or 3) a quarter $I_{\text{loss}} = 0.25$, of the information in the channel. The double column formation is used since it is simple and can therefore clearly reflect what happens (e.g., queue changes) in the event of communication loss. The plots of the errors for the different P_{txloss} when $I_{\text{loss}} = 0.50$ are shown in Fig. 14.

The spikes in the graphs occur when communication links are lost and the robots at the receiving end of the information decide

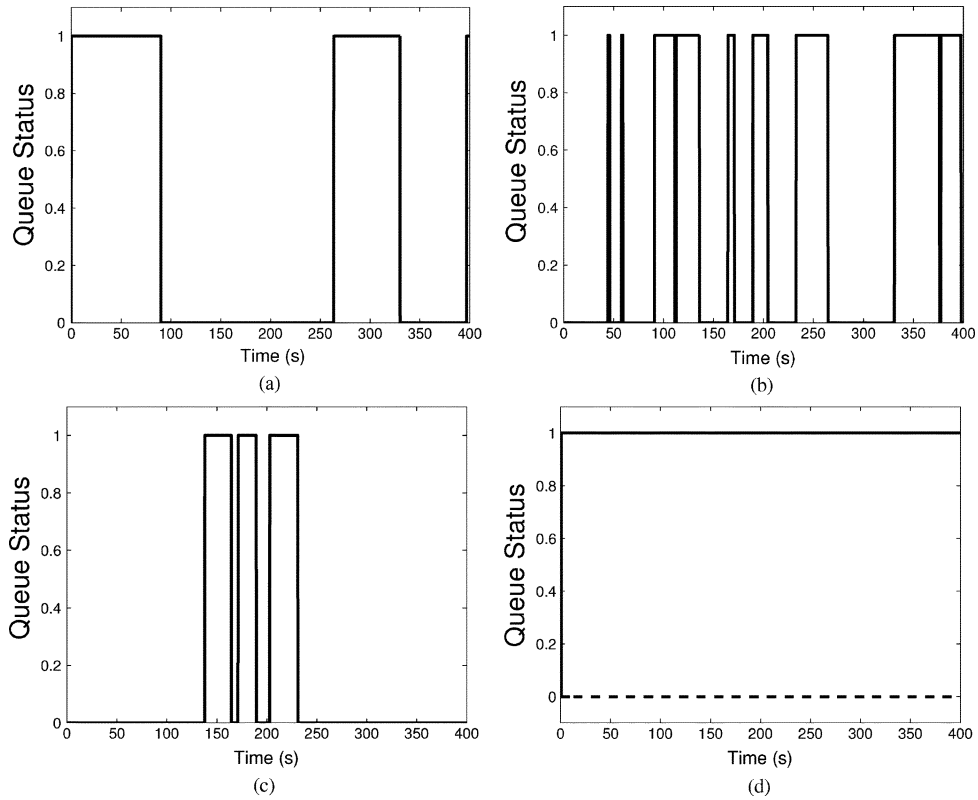

Fig. 15. Queue status of the robots for $I_{\text{loss}} = 0.50$, $P_{\text{txloss}} = 0.05$. (a) r_1. (b) r_7. (c) r_8. (d) Dash: r_2, r_5, r_6, r_9; solid: r_3, r_4.

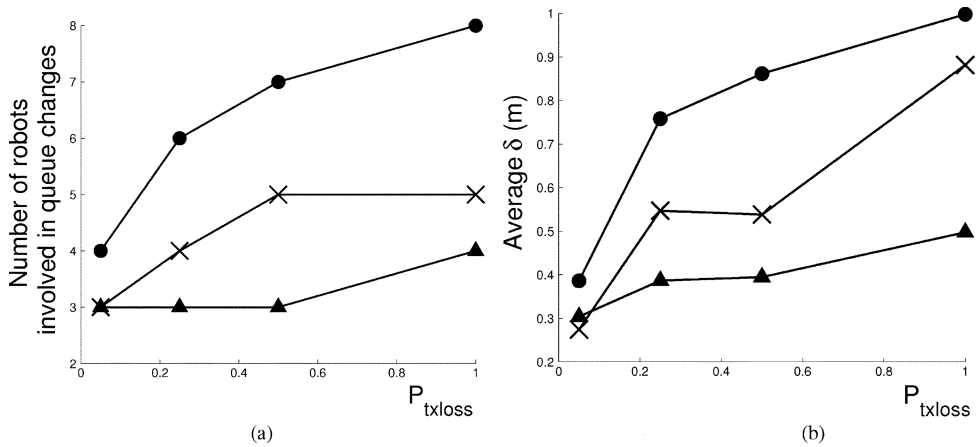

Fig. 16. Effect of different degrees of communication breakdown on the formation. Circle (•): $I_{\text{loss}} = 1.00$; cross (×): $I_{\text{loss}} = 0.50$; triangle (▲): $I_{\text{loss}} = 0.25$. (a) Number of robots involved in queue changes. (b) Average error in formation.

to change queue. For most cases, the team continues in formation, with those at the end of the queues toggling between the queues, causing the error δ. For $I_{\text{loss}} = 0.50$ with $P_{\text{txloss}} = 5\%$, the queue status of the robots are shown in Fig. 15. From the figure, we see that only robots r_1, r_7, and r_8 change their queue status frequently. Other robots are at the front of their queues, and will still detect another robot in their queue that is further from the formation vertex, and thus retain their queue status. The graphs in Fig. 16 show the number of robots involved in frequent toggling between queues, and the average error in the formation over the simulation time interval for different P_{txloss} and I_{loss}. As expected, extreme communication failure causes robots to constantly switch between queues, resulting in unstable formations.

VI. Conclusion and Future Work

A novel method for representing formation structures in terms of queues has been proposed to support a wide variety of formations, without requiring explicit representation of every single node. Together with the newly introduced artificial potential trenches, the scalability of formations is improved. Furthermore, formations are protected against failures of individual robots, and the group formation scales and adapts automatically. With the use of the IG method, the local minima problem due to the presence of deep crevices can be effectively addressed. However, it is noted that communications bandwidth places an upper bound on the maximum team size. Transmission fidelity also influences the stability of a formation.

In addition, there are several interesting issues that would benefit from more extensive research in the future. These include: 1) mathematical proofs relating to the stability of formations under the proposed scheme, drawing on stability concepts in control theory; 2) path planning and control of nonholonomic vehicles in response to forces generated by robot behaviors; and 3) communication issues that may provide insight into ways to reduce the reliance on extensive communications.

ACKNOWLEDGMENT

The authors would like to thank the Editor, S. Hutchinson, the Associate Editor, L. Parker, as well as the anonymous reviewers for their valuable comments and suggestions for improving earlier versions of this paper.

REFERENCES

[1] L. E. Parker, "ALLIANCE: An architecture for fault tolerant multirobot cooperation," *IEEE Trans. Robot. Autom.*, vol. 14, no. 2, pp. 220–240, Apr. 1998.
[2] B. P. Gerkey and M. J. Matarić, "Sold!: Auction methods for multirobot coordination," *IEEE Trans. Robot. Autom.*, vol. 18, no. 5, pp. 758–768, Oct. 2002.
[3] C. Fua, S. S. Ge, and K. W. Lim, "BOAs: Back-off adaptive scheme for task allocation with fault tolerance and uncertainty management," in *Proc. Int. Symp. Intell. Control*, Sep. 2004, pp. 162–167.
[4] T. Balch and M. Hybinette, "Social potentials for scalable multi robot formations," in *Proc. IEEE Int. Conf. Robot. Autom.*, Apr. 2000, pp. 73–80.
[5] S. Carpin and L. E. Parker, "Cooperative leader following in a distributed multi-robot system," in *Proc. IEEE Int. Conf. Robot. Autom.*, May 2002, pp. 2994–3001.
[6] P. Kostelnik, M. Šamulka, and M. Jánošík, "Scalable multi-robot formations using local sensing and communication," in *Proc. 3rd Int. Workshop Robot Motion and Control*, Nov. 2002, pp. 319–324.
[7] W. Kang, N. Xi, Y. Zhao, J. Tan, and Y. Wang, "Formation control of multiple autonomous vehicles: Theory and experimentation," in *Proc. IFAC 15th Triennial World Congr.*, 2002, pp. 1155–1160.
[8] R. O. Saber, W. B. Dunbar, and R. M. Murray, "Cooperative control of multi-vehicle systems using cost graphs and optimization," in *Proc. Amer. Control Conf.*, vol. 3, Jun. 2003, pp. 2217–2222.
[9] N. E. Leonard and E. Fiorelli, "Virtual leaders, artificial potentials, and coordinated control of groups," in *Proc. IEEE Conf. Decision and Control*, vol. 3, Dec. 2001, pp. 2968–2973.
[10] T. Balch and R. C. Arkin, "Behavior-based formation control for multirobot teams," *IEEE Trans. Robot. Autom.*, vol. 14, no. 6, pp. 926–939, Dec. 1998.
[11] A. K. Das, R. Fierro, V. Kumar, J. P. Ostrowski, J. Spletzer, and C. J. Taylor, "A vision-based formation control framework," *IEEE Trans. Robot. Autom.*, vol. 18, no. 5, pp. 813–825, Oct. 2002.
[12] J. P. Desai, J. P. Ostrowski, and V. Kumar, "Modeling and control of formations of nonholonomic mobile robots," *IEEE Trans. Robot. Autom.*, vol. 17, no. 6, pp. 905–908, Dec. 2001.
[13] M. Egerstedt and X. Hu, "Formation constrained multi-agent control," *IEEE Trans. Robot. Autom.*, vol. 17, no. 6, pp. 947–951, Dec. 2001.
[14] W. Ren and R. W. Beard, "A decentralized scheme for spacecraft formation flying via the virtual structure approach," *AIAA J. Guid., Control, Dynam.*, vol. 27, no. 1, pp. 73–82, Jan. 2004.
[15] M. Tillerson, L. Breger, and J. P. How, "Distributed coordination and control of formation flying spacecraft," in *Proc. Amer. Control Conf.*, vol. 2, Jun. 2003, pp. 1740–1745.
[16] T. Eren, P. N. Belhumeur, and A. S. Morse, "Closing ranks in vehicle formations based on rigidity," in *Proc. IEEE Conf. Decision and Control*, Dec. 2002, pp. 2959–2964.
[17] P. Song and V. Kumar, "A potential field based approach to multirobot manipulation," in *Proc. IEEE Int. Conf. Robot. Autom.*, May 2002, pp. 1217–1222.
[18] H. G. Tanner, G. J. Pappas, and V. Kumar, "Leader-to-formation stability," *IEEE Trans. Robot. Autom.*, vol. 20, no. 3, pp. 443–455, Jun. 2004.
[19] P. Ögren and N. E. Leonard, "Obstacle avoidance in formation," in *Proc. IEEE Int. Conf. Robot. Autom.*, Sep. 2003, pp. 2492–2497.
[20] S. S. Ge, C. Fua, and K. W. Lim, "Multirobot formations: Queues and artificial potential trenches," in *Proc. Int. Conf. Robot. Autom.*, Apr. 2004, pp. 3345–3350.
[21] R. O. Saber and R. M. Murray, "Flocking with obstacle avoidance: Cooperation with limited communication in mobile networks," in *Proc. IEEE Conf. Decision and Control*, vol. 2, Dec. 2003, pp. 2022–2028.
[22] S. S. Ge and Y. J. Cui, "New potential functions for mobile robot path planning," *IEEE Trans. Robot. Autom.*, vol. 16, no. 5, pp. 615–620, Oct. 2000.
[23] ——, "Dynamic motion planning for mobile robots using potential field method," *Auton. Robots*, vol. 13, pp. 207–222, 2002.
[24] S. S. Ge, Y. J. Cui, and C. Zhang, "Instant-goal-driven methods for behavior-based mobile robot navigation," in *Proc. IEEE Int. Symp. Intell. Control*, 2003, pp. 269–275.
[25] B. P. Gerkey, R. T. Vaughan, and A. Howard, "The player/stage project: Tools for multi-robot and distributed sensor systems," in *Proc. Int. Conf. Adv. Robot.*, Jun.–Jul. 2003, pp. 317–323.
[26] B. MacLennan, "Synthetic ethology: An approach to the study of communication," in *Artif. Life II: Proc. 2nd Workshop Synthesis and Simulation of Living Syst.*, vol. 11, 1991, pp. 631–658.
[27] L. E. Parker, "Designing control laws for cooperative agent teams," in *Proc. Int. Conf. Robot. Autom.*, vol. 3, 1993, pp. 582–587.
[28] ——, "The effect of action recognition and robot awareness in cooperative robotic teams," in *Proc. Int. Conf. Intell. Robots Syst.*, vol. 1, Aug. 1995, pp. 212–219.

Shuzhi Sam Ge (S'90–M'92–SM'00) received the B.Sc. degree from Beijing University of Aeronautics and Astronautics (BUAA), Beijing, China, in 1986, and the Ph.D. degree and the Diploma of Imperial College (DIC) from the Imperial College of Science, Technology, and Medicine, University of London, London, U.K., in 1993.

He has been with the Department of Electrical and Computer Engineering, National University of Singapore, Singapore, since 1993, where he is currently a Professor. He has authored and coauthored over 200 international journal and conference papers and three monographs, and coinvented three patents. He has been serving as the (Associate) Editor of several leading international journals. He has also been serving as a technical consultant for the local industry. His current research interests are control of nonlinear systems, neural/fuzzy systems, robotics, hybrid systems, sensor fusion, and system development.

Dr. Ge was the recipient of the 1999 National Technology Award, the 2001 University Young Research Award, and the 2002 Temasek Young Investigator Award, Singapore.

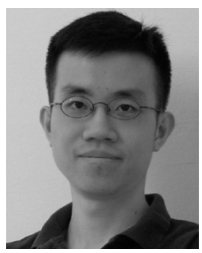

Cheng-Heng Fua (S'03) received the B.Eng. degree in electrical and computer engineering from the National University of Singapore (NUS), Singapore, in 2003, where he is currently working toward the Ph.D. degree in the Graduate School for Integrative Sciences and Engineering.

His research interests are in the area of autonomous multirobot collaboration and planning.

Mr. Fua is the recipient of the A∗Star Graduate Scholarship, awarded by the Agency for Science, Technology, and Research (A∗Star), Singapore.